A Vacuum Ultraviolet Photoionization Mass Spectrometric Study of Acetone

11 AUTHORS, INCLUDING:

Bin Yang
University of Oklahoma
29 PUBLICATIONS   802 CITATIONS

SEE PROFILE

Charles Chaoqun Huang
Wayland Baptist University
15 PUBLICATIONS   217 CITATIONS

SEE PROFILE

Xiaobin Shan
University of Science and Technology of China
46 PUBLICATIONS   298 CITATIONS

SEE PROFILE

Chow-shing Lam
University of Tennessee
18 PUBLICATIONS   182 CITATIONS

SEE PROFILE

A Vacuum Ultraviolet Photoionization Mass Spectrometric Study of Acetone

Lixia Wei, Bin Yang, Rui Yang, Chaoqun Huang, Jing Wang, Xiaobin Shan, Liusi Sheng, Yunwu Zhang, and Fei Qi*

National Synchrotron Radiation Laboratory, University of Science and Technology of China, Hefei, Anhui 230029, P. R. China

Chow-Shing Lam and Wai-Kee Li

Department of Chemistry, The Chinese University of Hong Kong, Shatin, N. T., Hong Kong

The photoionization and dissociative photoionization of acetone have been studied at the photon energy range of 8–20 eV. Photoionization efficiency spectra for ions $CH_3COCH_3^+$, CH_3^+, $C_2H_3^+$, $C_3H_3^+$, $C_3H_5^+$, CH_2CO^+, CH_3CO^+, $C_3H_4O^+$, and $CH_3COCH_2^+$ have been measured. In addition, the energetics of the dissociative photoionization has been examined by ab initio Gaussian-3 (G3) calculations. The computational results are useful in establishing the dissociation channels near the ionization thresholds. With the help of G3 results, the dissociation channels for the formation of the fragment ions CH_3CO^+, CH_2CO^+, CH_3^+, $C_3H_3^+$, and $CH_3COCH_2^+$ have been established. The G3 results are in fair to excellent agreement with the experimental data.

Introduction

As a common organic reagent, acetone is consumed in the manufacturing of methyl methacrylate and bisphenol A in industry. It is also extensively used as solvent. The ionization and dissociative properties of acetone have been studied by many groups using the method of electron impact ionization (EI)[1–5] as well as photoionization.[6–11]

Kanomata used EI to study the ionization and dissociation process of acetone with time-of-flight mass spectrometry (TOF–MS).[1] He obtained the ionization energy (IE) of acetone and the appearance energies (AEs) of fragment ions $m/e = 43$ (CH_3CO^+), 28 (CO^+), 27 ($C_2H_3^+$) and 15 (CH_3^+). He also calculated the AEs of different channels, but the calculated "values do not agree with the observed value."[1] Shigorin reported the AEs of fragment ions $m/e = 56$ ($C_3H_4O^+$) and 42 (CH_2CO^+) with EI method.[3] Other researchers reported only the IE of the molecule and the AE of fragment ion $m/e = 43$ (CH_3CO^+).[2,4,5] In short, the AEs obtained by EI are rather scattered. Moreover, little work has been done in establishing the dissociative channels of acetone.

Hurzeler et al. studied the ionization of acetone using a capillary discharge in hydrogen.[6] He reported the IE of acetone and the AE of fragment ion $m/e = 43$ (CH_3CO^+), while Edmond et al. further analyzed the dissociation channel of this fragmentation process.[7,8] Trott and co-workers also studied the analogous process of acetone as well as acetone-d_6 using a capillary discharge.[10] They observed a difference in the AEs of CH_3CO^+ and CD_3CO^+, due to isotope effect. Staley[9] and Traeger[11] reported the IE of acetone and AE of the fragment ion $m/e = 43$ (CH_3CO^+) as well. The AE value of CH_3CO^+ reported by Trott and co-workers is fractionally higher than those of others. It is noted that no AEs of other fragment ions have been reported using the method of photoionization. Consequently, no other channels have been studied. Powis et al. studied the PE of

acetone. They obtained the AE of fragment ions of $m/e = 43$ (CH_3CO^+) and $m/e = 15$ (CH_3^+) and analyzed the kinetic energy release in their results.[12] Still, they only reported the main ions and did not analyze the channels.

In the present work, we report the photoionization efficiency (PIE) curves of some additional ions resulting from the dissociative photoionization of acetone in the photon energy region of 8–20 eV. From these PIE data, we can derive the energetics of the dissociations. Combining these results with high level ab initio calculations, the various dissociation channels of acetone can be established.

Experimental and Theoretical Methods

The experimental and computational techniques employed in this work have been used to study the dissociations of ammonia,[13] vinyl chloride,[14] dichlorodifluoromethane,[15] carbon tetrachloride,[16] and ethylene oxide.[17] A brief description of these techniques is given below.

Experimental Method. The experimental setup has been described elsewhere,[13–17] and it is briefly outlined here. Synchrotron radiation from the 800 MeV electron storage ring of the National Synchrotron Radiation Laboratory, China, was monochromized by using a 1 m Seya-Namioka monochromator equipped with two gratings (2400 and 1200 lines/mm) covering the wavelength range from 40 to 200 nm. The wavelength of the monochromator was calibrated with the known IEs of the inert gases. The wavelength resolution is about 0.2 nm at the wavelength of 100 nm with 120 μm entrance and exit slits. The photon flux was monitored by a silicon photodiode (SXUV-100, International Radiation Detectors, Inc.). A LiF window (1.0 mm thickness) was used to eliminate higher order radiation of the dispersed light in the wavelength region longer than 105 nm.

A reflectron time-of-flight (RTOF) mass spectrometer was employed for the VUV photoionization/fragmentation studies. Photoions produced by the VUV light were drawn out of the

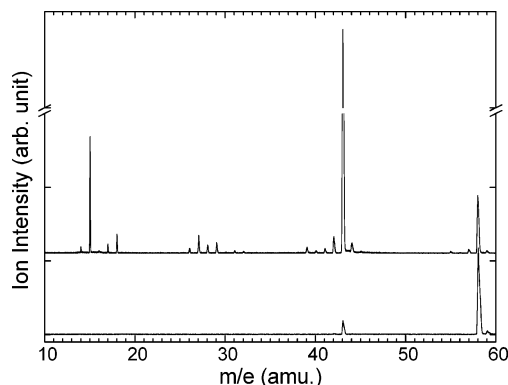* To whom correspondence should be addressed. E-mail: fqi@ustc.edu.cn.

Figure 1. Photoionization mass spectrum of acetone at the wavelength of 51.0 nm (24.31 eV, upper curve) and 110.0 nm (11.27 eV, lower curve).

Figure 2. Photoionization efficiency curve of mass 58 ($C_3H_6O^+$) from photoionization of acetone.

Figure 3. Photoionization efficiency curve of mass 43 (CH_3CO^+) from dissociative photoionization of acetone (10−11.25 eV).

Figure 4. Photoionization efficiency curve of mass 43 (CH_3CO^+) from dissociative photoionization of acetone (11.5−17.5 eV).

photoionization region by a pulse extraction field triggered with a pulse generator (DG 535, SRS) and detected by a microchannel plate (MCP) detector. The ion signal was recorded by a multiscaler P7888 (FAST Comtec, Germany) after it was amplified with preamplifier VT120C (EG & G, ORTEC). The total length of the ion flight is 1400 mm. The PIE curve was measured as the wavelength with increment of 0.2 nm.

The vapor of acetone (purity 99%) was introduced by supersonic expansion through a continuous beam nozzle with an orifice of 70 μm diameter from the molecular beam chamber into the ionization chamber through a 1.0 mm skimmer. In this experiment, He (purity 99.99%) was used as the carrier gas and the stagnation pressure was about 0.1 MPa. The pressure of the ionization chamber was about 4.2×10^{-4} Pa when the molecule beam was introduced. No cluster was observed under this condition, so no fragment ions were considered to originate from cluster dissociation.

Computational Method. The high level ab initio method employed in this work was the Gaussian-3 (G3) procedure, which is an approximation for the QCISD(T)/G3large energy. It involves single-point calculations at the MP4/6-31G(d), MP4/6-31+G(d), MP4/6-31G(2df,p), and MP2(Full)/G3large levels, all carried out with the structures optimized at the MP2(Full)/6-31G(d) level. The MP2(Full)/6-31G(d) harmonic frequencies, scaled by 0.9661, were used for correction of zero-point vibrational energies (ZPVE). A small semiempirical correction was also applied to account for the high level correlation effect. We have applied this method to study the structure, stability and reactivity of a variety of chemical systems.[18−22] The agreement between G3 energetics and experimental results is usually well within 0.15 eV. All the computations involved in this work were carried out on various workstations and PCs using the Gaussian03 suite of programs.[23]

Results and Discussion

Experimental Measurements. The photoionization mass spectrum of acetone at the wavelength of 51.0 nm is shown in Figure 1, together with that at 110.0 nm. The latter was obtained with a LiF window to eliminate higher order radiation. As can be seen from the figure, in addition to the parent ion $C_3H_6O^+$ and the fragment ions $C_2H_3O^+$ and CH_3^+, other smaller fragment ions can also be identified. The small peaks at $m/e = 17$, 18, 28, and 32 were observed because they come from the photoionization of background water and air. However, these peaks do not affect our attempt to establish the dissociation channels of acetone.
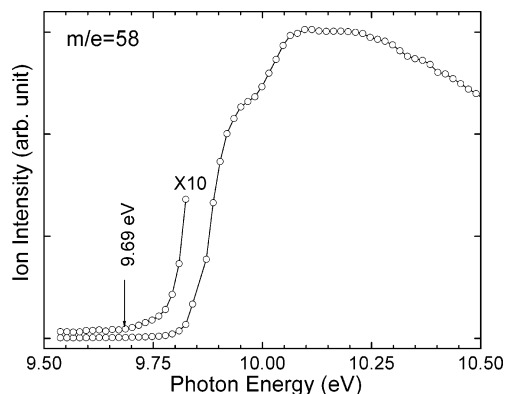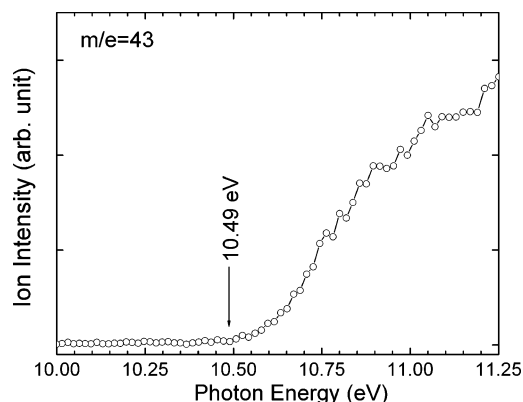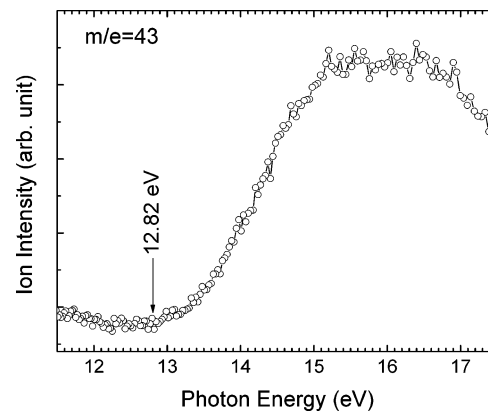
The PIE curves of the parent ion $C_3H_6O^+$ and of the fragment ions $C_2H_3O^+$, CH_3^+, $C_3H_5O^+$, $C_2H_3^+$, C_2HO^+, and $C_2H_2O^+$ from acetone were then measured. Figures 2−5 show the PIE spectra of the parent ion ($C_3H_6O^+$), the fragment ions $C_2H_3O^+$ (low energy region), $C_2H_3O^+$ (high energy region), and CH_3^+, respectively. The appearance energy (AE) was determined by the onset in each PIE curve. It should be pointed out that we ignored the thermal energy distribution of the parent molecule in our data treatment, considering the present nozzle expansion condition described above. In addition, no correction was made for possible kinetic shifts in determining the AEs.

All the AEs obtained from the PIE curves are listed in Table 1, along with the values measured by other researchers. The measurement error bars are also tabulated. The IE of $CH_3COCH_3^+$ and AE of CH_3CO^+ that we report here are very close

Photoionization Study of Acetone

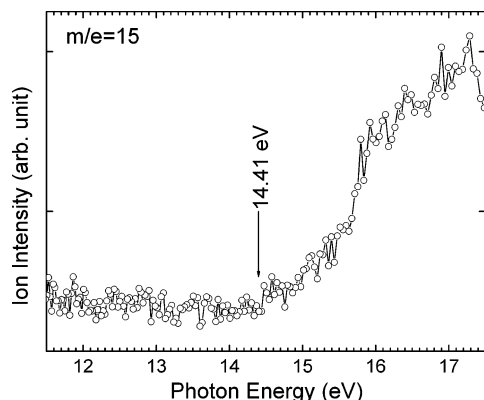*J. Phys. Chem. A, Vol. 109, No. 19, 2005* **4233**

Figure 5. Photoionization efficiency curve of mass 15 (CH_3^+) from dissociative photoionization of aceton.

TABLE 1: Appearance Energies (eV) Measured in the Dissociative Photoionizations of Acetone

m/e	ion	this work	PI[a]	EI[b]
15	CH_3^+	14.41 ± 0.04		15.53 ± 0.08
27	$C_2H_3^+$	15.59 ± 0.04		16.9
39	$C_3H_3^+$	14.51 ± 0.03		
41	C_2HO^+	15.63 ± 0.04		
42	CH_2CO^+	10.53 ± 0.02		10.7 ± 0.1^c
		14.97 ± 0.04		
43	CH_3CO^+	10.49 ± 0.02	10.52 ± 0.02^d	10.94 ± 0.04^e
		12.82 ± 0.03		
56	$C_3H_4O^+$	12.71 ± 0.03		15.2 ± 0.15^f
57	$CH_3COCH_2^+$	13.10 ± 0.03		
58	$CH_3COCH_3^+$	9.69 ± 0.02	9.694 ± 0.006^g	9.84 ± 0.04^h

^{a} Data taken from ref 10. ^{b} Data taken from ref 1. ^{c} Data taken from ref 3. ^{d} Other reported values (in eV) for this ion include 10.37 (ref 8), 10.36 (ref 9), and 10.38 (ref 11). ^{e} Other reported values (in eV) for this ion include 10.2 ± 0.1 (ref 2) and 10.30 (ref 4). ^{f} Data taken from ref 3. ^{g} Other reported values (in eV) for the molecule ion include 9.690 ± 0.01 (ref 5), 9.65 ± 0.1 (ref 6), 9.68 ± 0.02 (ref 7), and 9.68 (ref 9). ^{h} Other reported values (in eV) for the molecule ion include 9.7 ± 0.1 (ref 2) and 9.71 ± 0.03 (ref 4).

to those obtained by using the photoionization method but lower than those obtained by the EI ionization method. This is understandable since the EI ionization method often overestimates the IE of the parent molecule and the AEs of the fragment ions. It should be pointed out that, in measuring the IE of C_3H_6O and the AEs of $C_2H_3O^+$ and $C_2H_2O^+$ from acetone in the low energy range, a LiF filter was used to eliminate the effect of higher order radiation from the grating. Our photoionization onset in the PIE curve of parent ion $C_3H_6O^+$ in Figure 2 appears quite sharp and clear. In addition, our experiments were carried out under supersonic cooling conditions, thereby overcoming the hot band effect and other influences on the accurate determination of the AEs. Also, the light source employed was high-intensity synchrotron radiation. We therefore believe that the IE of acetone we have obtained is more accurate than those of the previous measurements. For the fragment ions $m/e = 42$ (CH_2CO^+) and 43 (CH_3CO^+), two onsets were observed from PIE measurement. Field-induced dissociative ionization and kinetic shift cannot have a serious effect ($\sim 0.002-0.005$ eV) here, compared to the dissociation energies discussed in this article.[24,25]
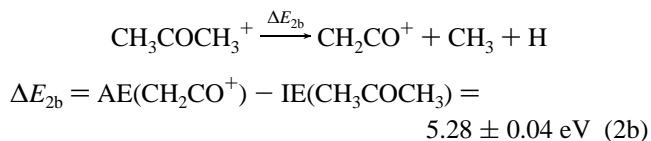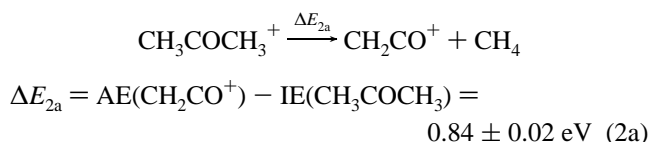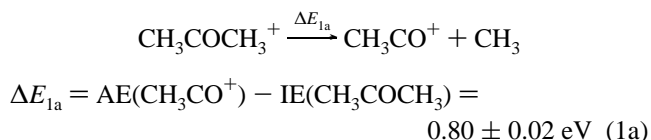
Computational Results. The structural formulas of the polyatomic species (with more than three atoms) involved in this work, along with their symmetry point groups and electronic states, are displayed in Figure 6. The calculated G3 energies of various species involved in the dissociations of acetone and its

cation are summarized in Table 2. With the aid of these results, we have established the dissociation channels of the acetone cation.

With the E_0(G3) values of CH_3COCH_3 and $CH_3COCH_3^+$, the IE of acetone is calculated to be 9.74 eV. Considering that the error range of G3 results is ± 0.15 eV, this calculation value is in good agreement with the experimental result, 9.69 ± 0.02 eV.

Dissociation Channels of Acetone Cation. Dissociations of the acetone cation, which involve either only the cleavage of bond(s) or transition structure(s), are discussed in this section.

(1) $m/e = 42$ (CH_2CO^+), 43 (CH_3CO^+). Because of its lack of γ-H, acetone undergoes a Norrish I dissociation. In fact, such a channel is typical of ketones with a methyl group connected to the carbonyl and it is always the major one, especially in the case of acetone. Cations CH_3CO^+ and CH_2CO^+ may be generated through the following reactions:

$$CH_3COCH_3^+ \xrightarrow{\Delta E_{1a}} CH_3CO^+ + CH_3$$

$$\Delta E_{1a} = AE(CH_3CO^+) - IE(CH_3COCH_3) = 0.80 \pm 0.02 \text{ eV} \quad (1a)$$

$$CH_3COCH_3^+ \xrightarrow{\Delta E_{2a}} CH_2CO^+ + CH_4$$

$$\Delta E_{2a} = AE(CH_2CO^+) - IE(CH_3COCH_3) = 0.84 \pm 0.02 \text{ eV} \quad (2a)$$

$$CH_3COCH_3^+ \xrightarrow{\Delta E_{2b}} CH_2CO^+ + CH_3 + H$$

$$\Delta E_{2b} = AE(CH_2CO^+) - IE(CH_3COCH_3) = 5.28 \pm 0.04 \text{ eV} \quad (2b)$$

In the above mathematical expressions, we use our experimental IE and AEs. The dissociation energies, along with those calculated by the G3 method (using the results given in Table 2), are tabulated in Table 3 for easy comparison.

The energy profiles of these three reactions are displayed in Figure 7. It is seen that there is a transition structure (TS), **TS-(1→2)**, for both reactions. In this TS, the length of the C−C bond that is about to be cleaved is about 2.27 Å. The G3 energy of **TS(1→2)** is 0.59 eV above that of the parent ion $CH_3COCH_3^+$(**1**), while the energy of the dissociated products **3a** and **3b** (calculated from results listed in Table 2) is 0.83 eV higher than that of **1**. In other words, this TS has an energy lower than that of its products. Nevertheless, reaction 1a can still be described as a dissociation mediated by ion−neutral complex (INC). In this type of reactions, the INC involved is not necessarily a local minimum on the potential surface. It is said to be located in an *entropy well* provided by the increased internal rotational degrees of freedom.[26,27] Therefore, ion-radical complex (IRC) **2**, like other INCs in numerous reactions, can be accepted as an intermediate and capable of undergoing subsequent reactions, such as reaction 2a in which hydrogen abstraction via **TS(2→4)** takes place (to be discussed below). In any event, the G3 dissociation energy for reaction 1a is 0.83 eV, in very good agreement with the experimental result, 0.80 ± 0.02 eV.

To yield CH_2CO^+ and CH_4 in reaction 2a, parent ion **1** first undergoes a process of C−C bond cleavage via **TS(1→2)** to form IRC **2** (structure shown in Figure 6). Then IRC **2** undergoes a methyl migration followed by a hydrogen abstraction to produce CH_2CO^+(**4a**) and CH_4(**4b**) via **TS(2→4)**. The calculated
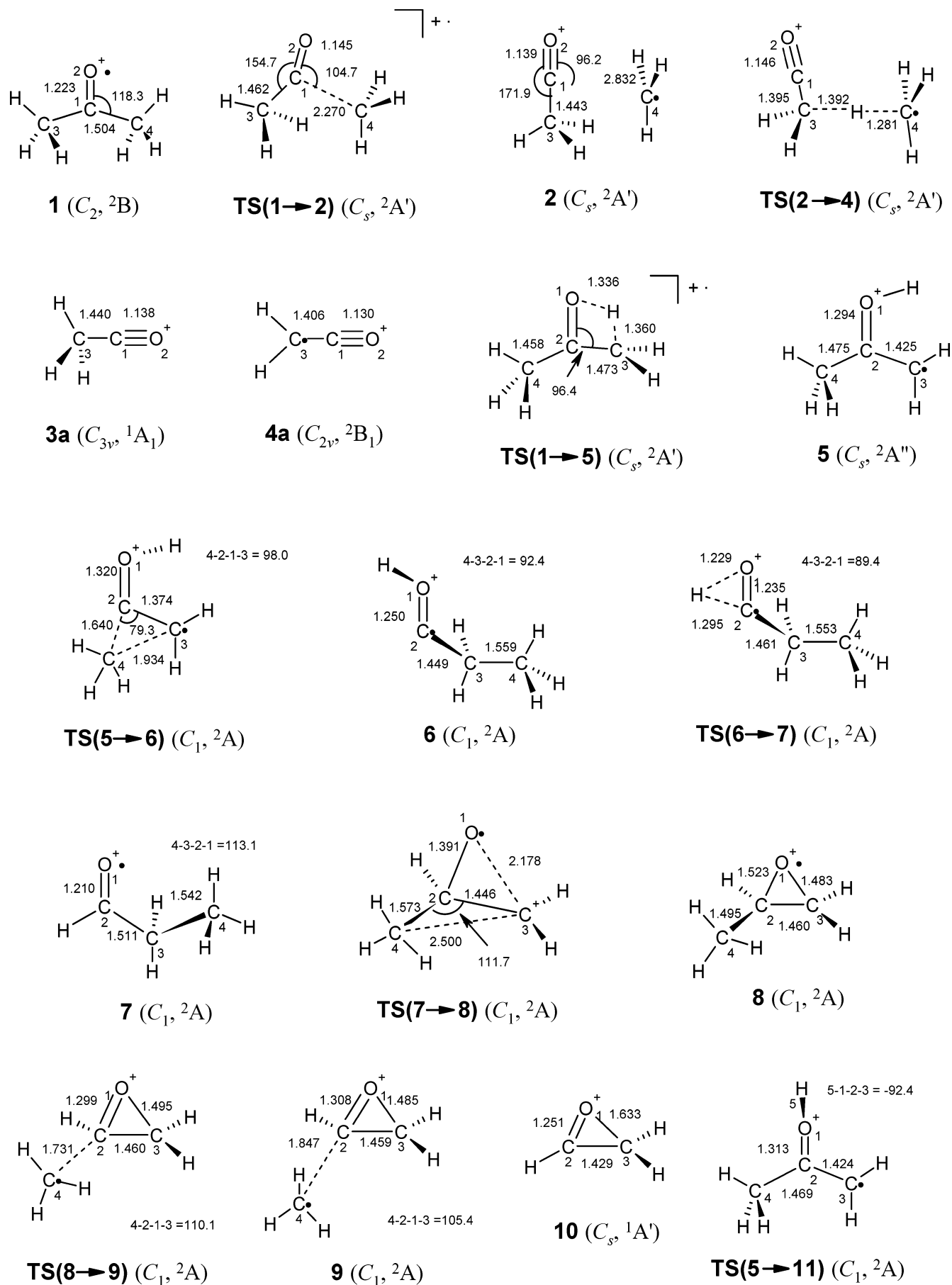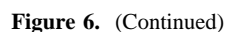
1 (C_2, ^{2}B)

TS(1→2) (C_s, ^{2}A′)

2 (C_s, ^{2}A′)

TS(2→4) (C_s, ^{2}A′)

3a (C_{3v}, ^{1}A$_1$)

4a (C_{2v}, ^{2}B$_1$)

TS(1→5) (C_s, ^{2}A′)

5 (C_s, ^{2}A″)

TS(5→6) (C_1, ^{2}A)

6 (C_1, ^{2}A)

TS(6→7) (C_1, ^{2}A)

7 (C_1, ^{2}A)

TS(7→8) (C_1, ^{2}A)

8 (C_1, ^{2}A)

TS(8→9) (C_1, ^{2}A)

9 (C_1, ^{2}A)

10 (C_s, ^{1}A′)

TS(5→11) (C_1, ^{2}A)

Figure 6.

Photoionization Study of Acetone

J. Phys. Chem. A, Vol. 109, No. 19, 2005 **4235**
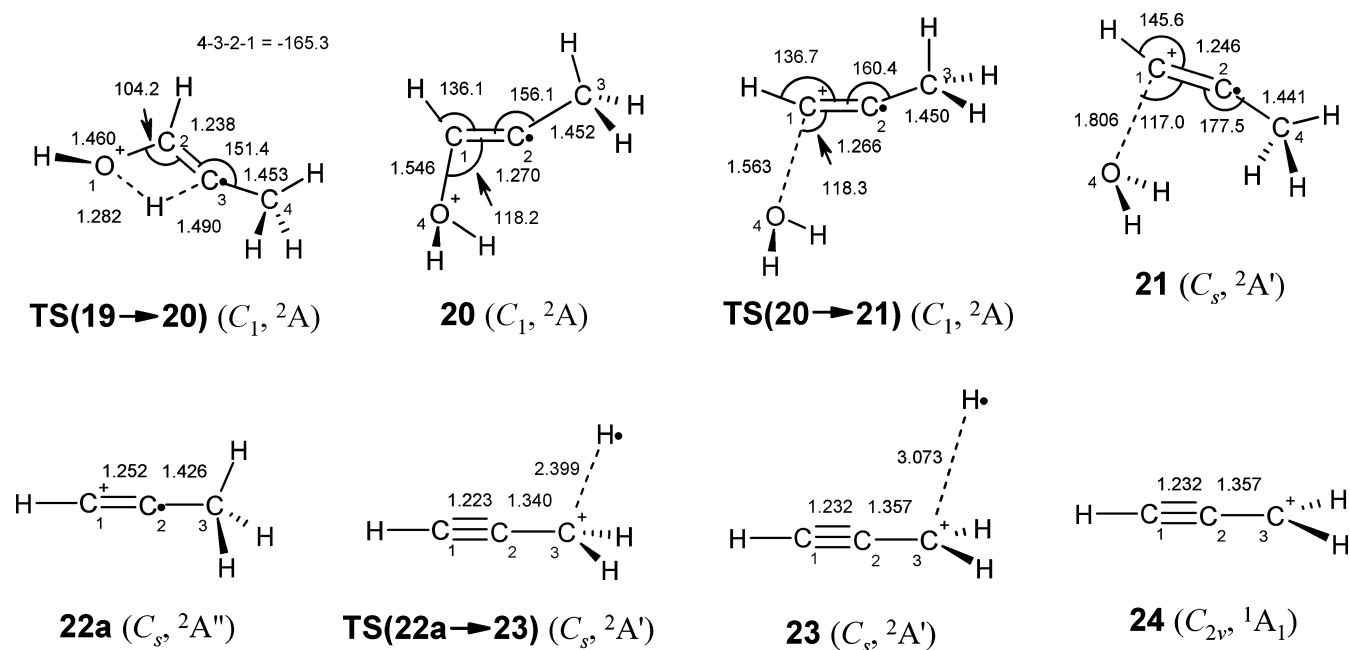

Figure 6. (Continued)

Figure 6. Structural formulas of the various polyatomic species (with more than three atoms) involved in this work, along with their symmetry point groups and electronic states.

barrier of reaction 2a is 0.84 eV, in excellence agreement with the experimental dissociation energy, 0.84 ± 0.02 eV.

For ion with $m/e = 42$, another onset was observed at 14.97 ± 0.04 eV. This requires another dissociation channel that would produce ion **4a**. Our G3 results suggest a pathway in which **4a** is formed via loss of a hydrogen atom from **3a**, involving no TS. This pathway is summarized in Figure 7. The G3 dissociation energy is found to be 5.27 eV, also in excellent agreement with the experimental value of 5.28 ± 0.04 eV.

(2) $m/e = 43$ (c-CH$_3$CO$^+$) and $m/e = 15$ (CH$_3^+$). The dissociation channels described above are rather simple involving no rearrangement. However, another onset also observed at $m/e = 43$ requires a more complex dissociation channel.

$$CH_3COCH_3^+ \xrightarrow{\Delta E_{1b}} c\text{-}CH_3CO^+ + CH_3$$
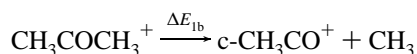
$$\Delta E_{1b} = AE(c\text{-}CH_3CO^+) - IE(CH_3COCH_3) =$$
$$3.13 \pm 0.03 \text{ eV} \quad (1b)$$

Computational results suggest a pathway in which a cyclic CH$_3$CO$^+$ ion **10**, an isomer of **3a**, is produced in reaction 1b. The energy profile of this reaction is shown in Figure 8. In this profile, parent ion **1** undergoes a series of rearrangements which deserve a fuller description. First, ion **1** undergoes a hydrogen atom transfer from a methyl group to the carbonyl oxygen via **TS(1→5)**. The G3 barrier for this step is 1.56 eV. This process produces ion **5** which is more stable than its parent ion **1** by 0.38 eV. Subsequently, ion **5** undergoes a methyl group transfer from the carbonyl carbon to the radical center via **TS(5→6)**, which is 1.82 eV higher than **1** in energy, to produce **6**, which is less stable than **1** by 0.86 eV. Afterward, ion **6** undergoes a hydrogen atom shift from oxygen to the carbonyl carbon via **TS(6→7)**. This TS is rather high in energy, and it is 2.38 eV above **1**. The intermediate formed is essentially a propanal radical cation **7**, which is less stable than **1** thermodynamically. The last rearrangement in this pathway takes place via **TS(7→8)**. This TS involves simultaneous methyl group transfer to the carbonyl center and a cyclization step forming an epoxide-like framework. It is worthy to note that in **TS(7→8)**, the positive

charge is localized on the sp^2 carbon according to our computational results. Therefore, the methyl group shift is actually a carbanion CH$_3^-$ transfer. On the other hand, the unpaired electron is localized on oxygen. So the cyclization process can be described as an intramolecular hydroxyl radical attack at the cationic carbon. More importantly, the CH$_3^-$ carbanion transfer is almost complete when the energy is at maximum on the potential energy surface. As shown in Figure 6, the newly formed C–C bond is as short as 1.57 Å, in the range of ordinary C–C single bond length. The energy of **TS-(7→8)** is the highest among the four rearrangement TSs; it is 2.96 eV above **1** in energy.

After these rearrangements, the radical cation of propylene oxide, species **8**, is produced. To yield product ion **10**, ion **8** undergoes a methyl group loss via **TS(8→9)**. Similar to the C–C bond cleavage in reaction 1a, this process is also mediated by IRC **9**, which is a complex formed by ion **10** and methyl radical **3b**. This complex is again energetically higher than the TS producing it; the G3 energy of IRC **9** is 0.30 eV higher than **TS(8→9)**. Dissociation of IRC **9** releases ion **10** and radical **3b** as final dissociation products. These products are highest in energy along the whole pathway and their total energy is 3.26 eV above parent ion **1**. This value is taken as the G3 dissociation energy, and it is in good accord with the experimental value of 3.13 ± 0.03 eV.

Three alternative pathways for the formation of $m/e = 43$ fragment ions are shown in Figure 9. One of the pathways shown in this figure is: **1 → TS(1→5) → 5 → TS(5→11) → 11 → TS(11→12) → 12 → 3c + 3b**. In this pathway, once **5** is formed, it undergoes a C–O π-bond rotation via **TS(5→11)**. From the structure of **TS(5→11)** shown in Figure 6, it can be seen that the C–O bond is slightly lengthened from 1.29 in **5** to 1.31 Å. This π-bond rotation has a barrier of 0.70 eV and this process yields ion **11**. Then **11** has its H$_3$C–C bond cleaved via **TS-(11→12)** to yield IRC **12**, which dissociates to produce protonated ketene **3c** and methyl radical **3b**. The step involving **TS(11→12)** entails a large barrier of 4.23 eV, which is much larger than the experimental result of 3.13 ± 0.03 eV. Hence this pathway may be safely ignored. Another pathway which

Photoionization Study of Acetone

J. Phys. Chem. A, Vol. 109, No. 19, 2005 **4237**

TABLE 2: G3 Energies E_0 and H_{298} (in hartrees) of Various Species Involved in the Dissociation of Acetone

species	E_0 (hartrees)	H_{298} (hartrees)
acetone	−192.99441	−192.98807
1	−192.63692	−192.63027
TS(1→2)	−192.61563	−192.60862
2	−192.61520	−192.60670
TS(2→4)	−192.60647	−192.59950
TS(1→5)	−192.57865	−192.57283
5	−192.65041	−192.64424
TS(5→6)	−192.56924	−192.56352
6	−192.60481	−192.59860
TS(6→7)	−192.54912	−192.54275
7	−192.61409	−192.60787
TS(7→8)	−192.52716	−192.52149
8	−192.57100	−192.56528
TS(8→9)	−192.55651	−192.55068
9	−192.54555	−192.53941
TS(5→11)	−192.62437	−192.61838
11	−192.65195	−192.64584
TS(11→12)	−192.48272	−192.47498
12	−192.56283	−192.55482
TS(6→13)	−192.60479	−192.59928
13	−192.60675	−192.60057
TS(13→3′)	−192.53915	−192.5321
TS(5→3)	−192.46830	−192.46101
TS(11→15)	−192.56121	−192.55538
15	−192.57106	−192.56527
TS(15→16)	−192.51493	−192.50889
TS(1→17)	−192.537	−192.53092
17	−192.53951	−192.53131
TS(1→16)	−192.51902	−192.51283
TS(11→16)	−192.51899	−192.51259
TS(15→18)	−192.47878	−192.47294
18	−192.56644	−192.56072
TS(18→19)	−192.56755	−192.56194
19	−192.64918	−192.64311
TS(19→20)	−192.53150	−192.52553
20	−192.57931	−192.57218
TS(20→21)	−192.57965	−192.57323
21	−192.58067	−192.57296
3a	−152.81695	−152.81240
3b	−39.79144	−39.78733
3c	−152.75129	−152.74657
TS(3a→3c)	−152.65921	−152.65452
4a	−152.15284	−152.14833
4b	−40.45548	−40.45167
4c	−0.50100	−0.50100
10	−152.72746	−152.72326
TS(10→3a)	−152.64445	−152.63962
14a	−39.42928	−39.42548
14b	−113.26765	−113.26388
16a	−192.03628	−192.03058
22a	−116.17208	−116.16684
22b	−76.38180	−76.37802
TS(22a→23)	−116.09228	−116.08638
23	−116.09317	−116.08604
24	−115.58993	−115.58495

TABLE 3: Experimental and Calculated (G3) Energies (eV) of the Dissociations of the Acetone Cation

dissociation reactions	ΔE(exp)	G3 reaction barrier
$C_3H_6O^+ \rightarrow CH_3CO^+ + CH_3$ (1a)	0.80 ± 0.02	0.83
or $CH_2CHO^+ + CH_3$ (1b)	3.13 ± 0.03	3.26
$C_3H_6O^+ \rightarrow CH_2CO^+ + CH_4$ (2a)	0.84 ± 0.02	0.84
or $CH_2CO^+ + CH_3 + H$ (2b)	5.28 ± 0.04	5.27
$C_3H_6O^+ \rightarrow CH_3^+ + CO + CH_3$ (3)	4.72 ± 0.04	4.61
$C_3H_6O^+ \rightarrow CH_3COCH_2^+ + H$ (4)	3.41 ± 0.03	3.30
$C_3H_6O^+ \rightarrow C_3H_3^+ + H_2O + H$ (5)	4.82 ± 0.03	4.94[a]

[a] This value is calculated at the CCSD(T)/G3large level without including ZPVE correction (see text for details).

methyl radical **3b**. In this pathway, once intermediate **5** is formed, its H_2C group breaks away from the carbonyl carbon and at the same time abstracts the hydrogen of the $C=O^+-H$ group via **TS(5→3)** to produce **3a** and **3b**. The overall barrier of this mechanism is so high (4.61 eV) that it is not likely to be of importance as far as producing $m/e = 43$ fragment ions is concerned. However, cation **3a** can cleave its C−C bond to yield CH_3^+ (**14a**) and CO (**14b**). The overall barrier of this process is 4.61 eV, in fair agreement with the experimental result of 4.72 ± 0.04 eV. In other words, the generation $m/e = 15$ fragment ions CH_3^+ can be summarized by the equation:

$$CH_3COCH_3^+ \xrightarrow{\Delta E_3} CH_3^+ + CO + CH_3$$
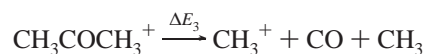
$$\Delta E_3 = AE(CH_3^+) - IE(CH_3COCH_3) =$$
$$4.72 \pm 0.04 \text{ eV} \quad (3)$$

To make the story complete, we have also investigated the possibility of producing **3c** by the isomerization of cation **10** or by the isomerization of **3a**. The G3 results of these processes are displayed in Figure 10. As shown there, we did locate a TS, **TS(3a→3c)** and its barrier of 5.13 eV. On the other hand, we were not successful in finding the TS for **10 → 3c**. Instead, we located a TS for the transformation of **10 → 3a**. This TS, called **TS(10→3a)**, involves simultaneous ring-opening and hydrogen shift and this barrier is 5.53 eV. In other words, to effect **10 → 3c**, we need to go by way of **3a**. Still, the barriers for **10 → 3a** and **3a → 3c** are much higher than the experimental AE of $m/e = 43$ ions, 3.13 ± 0.03 eV. Hence the processes shown in Figure 10 are merely of academic interest and they are not likely to take place in the photodissociation experiment.

(3) $m/e = 57$ ($CH_3COCH_2^+$). Intuitively, one may think that reaction 4, shown below, is a simple bond cleavage process. However, our calculations suggest a slightly more complicated mechanism, which is summarized by the energy profile shown in Figure 11.

$$CH_3COCH_3^+ \xrightarrow{\Delta E_4} CH_3COCH_2^+ + H$$
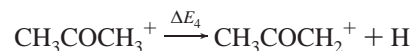
$$\Delta E_4 = AE(CH_3COCH_2^+) - IE(CH_3COCH_3) =$$
$$3.41 \pm 0.03 \text{ eV} \quad (4)$$

As described in Figure 9, ion **1** can undergo a series of isomerization steps to form intermediate **11** (this portion of the pathway is also displayed in Figure 11). Ion **11** can cyclize to form ion **15** with an epoxide-like framework via **TS(11→15)**. The G3 energy of **TS(11→15)** is higher than **1** by 2.04 eV. It is worth noting that ion **15**, being 1.77 eV above **1** in energy, is a cyclic distonic ion with a positive charge on oxygen and an unpaired electron on the carbon atom which is originally the carbonyl carbon. Finally, ion **15** dissociates into cyclic CH_3-
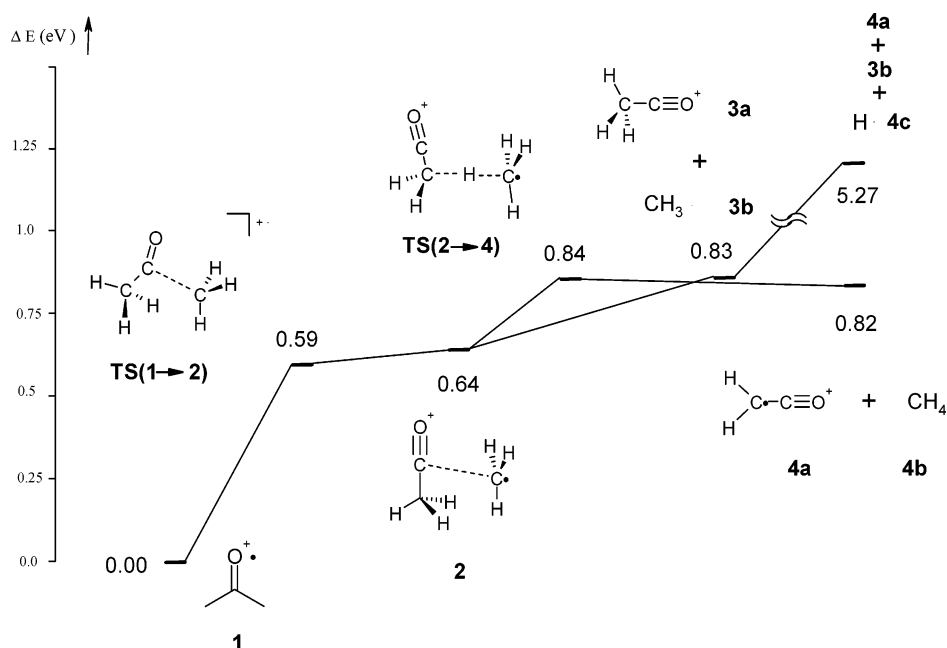
also produces **3c** shown in Figure 9 involves intermediate **6**. Once **6** is formed, it isomerizes to **13** via **TS(6→13)**. The G3 energy barrier for this C−CO bond rotation is quite small. Ion **13** can then cleave the H_3C-C bond via **TS(13→3′)** to produce again **3b** and **3c**. In this pathway, the final step is rate-determining, with a barrier of 2.67 eV. While this barrier is smaller than the overall barrier of the preferred pathway shown in Figure 8, we are of the opinion that, once intermediate **6** is formed, it is more likely to go through **TS(6→7)** (with a barrier of 2.38 eV, shown in Figure 8) than **TS(6→13)** → **13** → TS-**(13→3′)** (barrier being 2.67 eV). Still, with a relatively small barrier difference of 0.29 eV, the formation of protonated ketene **3c** cannot be entirely ruled out. Now we discuss the final pathway shown in Figure 9 which also produces cation **3a** and

Figure 7. Gaussian-3 potential energy surface showing the possible mechanism for reaction 1a, $CH_3COCH_3^+ \rightarrow CH_3CO^+ + CH_3$, reaction 2a, $CH_3COCH_3^+ \rightarrow CH_2CO^+ + CH_4$, and reaction 2b, $CH_3COCH_3^+ \rightarrow CH_2CO^+ + H + CH_3$.
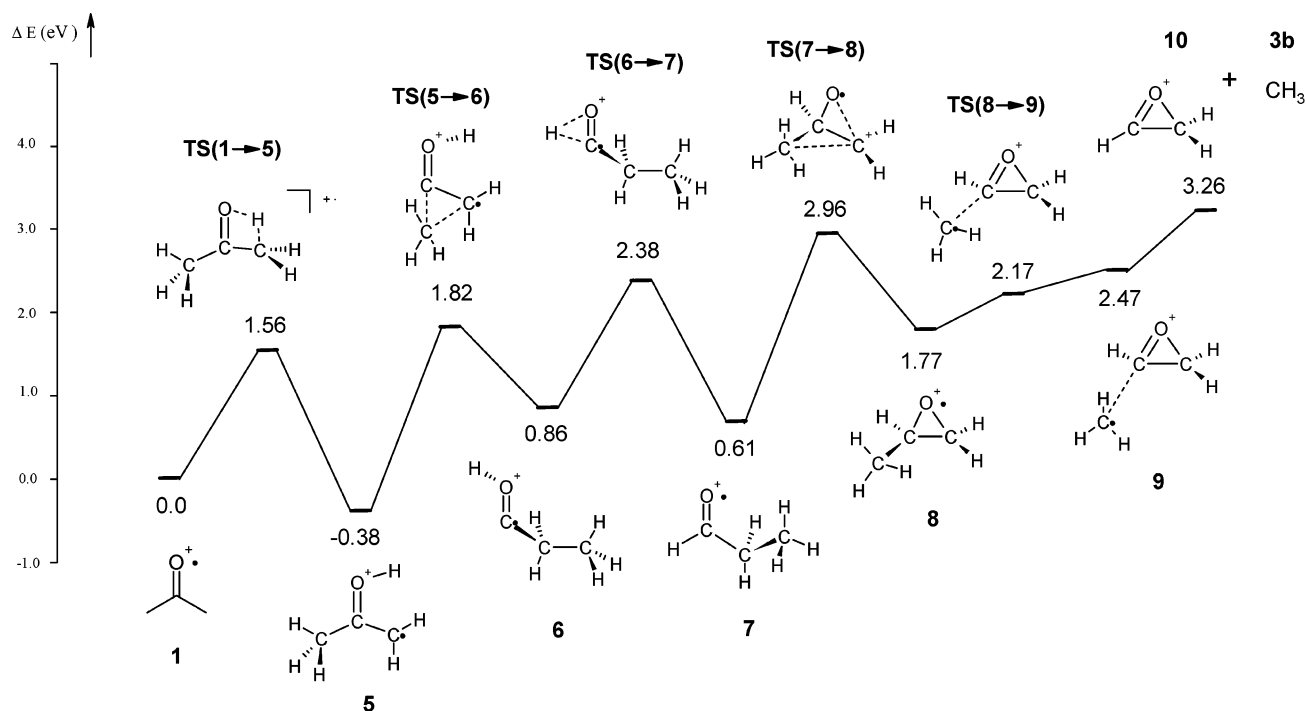

Figure 8. Gaussian-3 potential energy surface showing the possible mechanism for reaction 1b, $CH_3COCH_3^+ \rightarrow c\text{-}CH_3CO^+ + CH_3$.

$COCH_2^+$ (**16a**) and hydrogen atom (**4c**) via **TS(15→16)**, which is 3.30 eV above parent ion **1**. This value is taken as the G3 dissociation energy.

Referring to Figure 11, in addition to the proposed pathway **1 → TS(1→5) → 5 → TS(5→11) → 11 → TS(11→15) → 15 → TS(15→16) → 16a + 4c** discussed above, there are three alternative pathways that may also lead to the formation of m/e = 57 fragment ions. Two of them are direct C−H bond breaking processes. The TSs, namely **TS(1→17)** and **TS(1→16)**, are very similar; both involve simultaneous C−H bond breaking and ring closure. The respective barriers for these two pathways are 2.70 and 3.20 eV. Since these barriers are larger than that for **TS-(1→5)** (1.56 eV), reactant **1** is unlikely to go through **TS(1→17)**

or **TS(1→16)**; it should go through **TS(1→5)** instead. As shown in Figure 11, the last alternative pathway is: **1 → TS(1→5) → 5 → TS(5→11) → 11 → TS(11→16) → 16a + 4c**, with a barrier of 3.20 eV. Even though this barrier is slightly lower than that of our suggested pathway (3.30 eV) discussed in the previous paragraph, we do not think this is the preferred pathway. This is because, once intermediate **11** is formed, it is likely to go through **TS(11→15)** (with barrier 2.04 eV) than **TS(11→15)** (with barrier 3.20 eV). To summarize, the formation of m/e = 57 fragment ions (**16a**) and H has a G3 barrier of 3.30 eV, which is in good agreement with experimental value of 3.41 ± 0.03 eV. Finally, in passing, all three discarded pathways involve concomitant cyclization and C−H (or O−H) bond breaking at
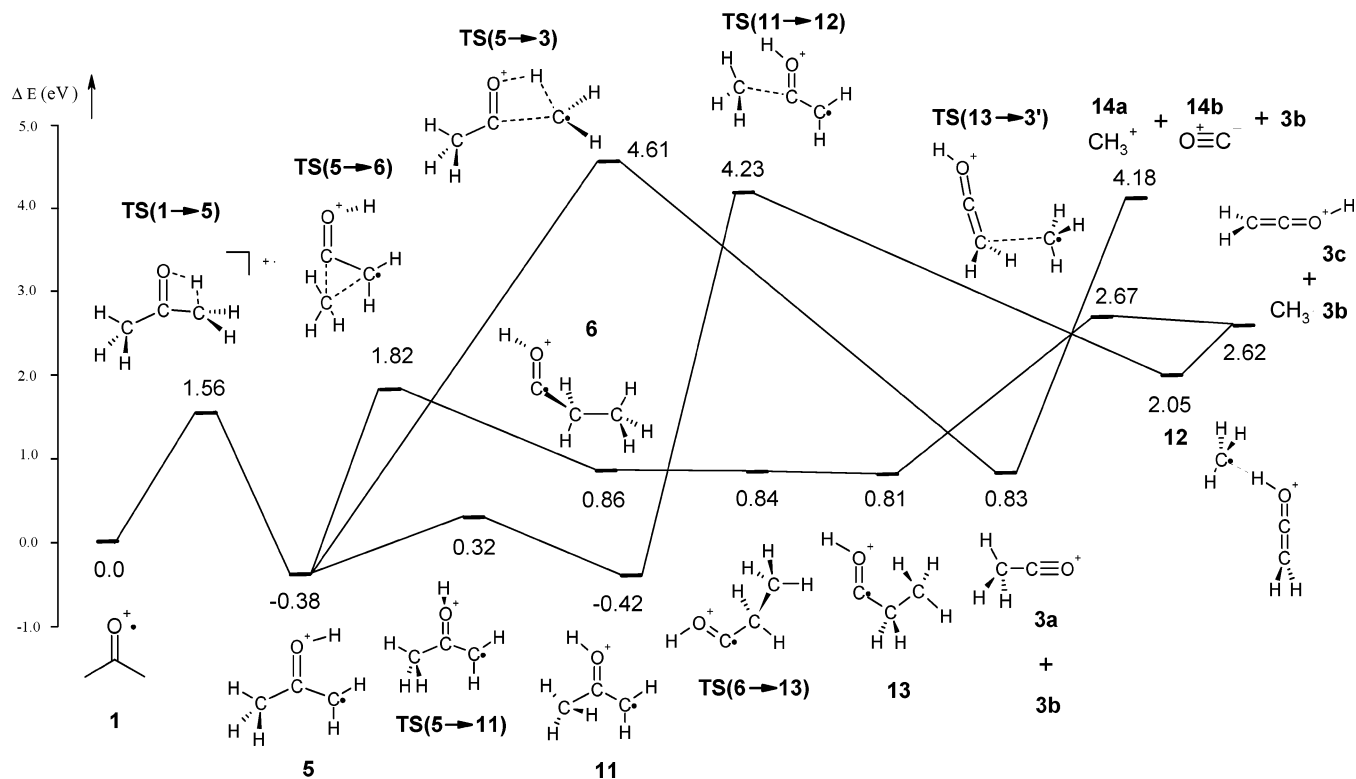
Photoionization Study of Acetone

J. Phys. Chem. A, Vol. 109, No. 19, 2005 **4239**

Figure 9. Gaussian-3 potential energy surface showing the possible mechanism for the reaction $CH_3COCH_3^+ \rightarrow CH_3CO^+$ (or CH_2COH^+) + CH_3 and reaction 3 $CH_3COCH_3^+ \rightarrow CH_3^+ + CO + CH_3$.
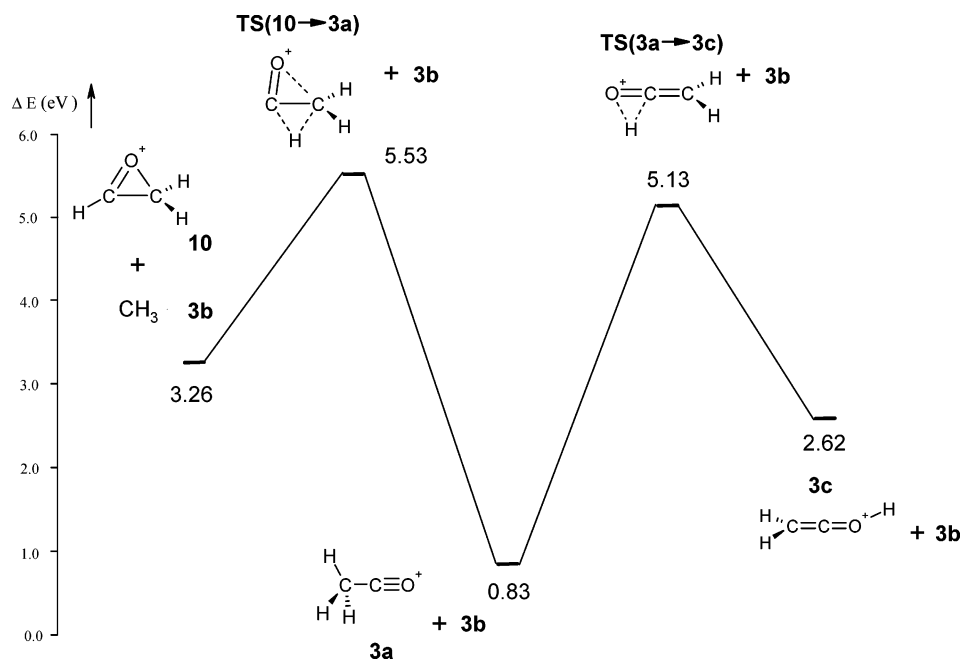

Figure 10. Gaussian-3 potential energy surface showing the possible mechanism for the isomerization reactions of $m/e = 43$ fragment ions.

TS(1→17), **TS(1→16)** or **TS(11→16)**. On the other hand, in the preferred process, cyclization takes place at **TS(11→15)** before the breaking of the O–H bond at **TS(15→16)**.

(4) $m/e = 39$ ($C_3H_3^+$). The following dissociation reaction yields cation $C_3H_3^+$:

$$CH_3COCH_3^+ \xrightarrow{\Delta E_5} C_3H_3^+ + H_2O + H$$
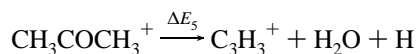
$$\Delta E_5 = AE(C_3H_3^+) - IE(CH_3COCH_3) = 4.82 \pm 0.03 \text{ eV} \tag{5}$$

The results of our calculations suggest that reaction 5 is branched from reaction 4. The energy profile of reaction 5 is displayed in Figure 12. To yield product ion $C_3H_3^+$ (**24**), ion **15**, which is one of the intermediates in reaction 4, undergoes a series of isomerization steps before elimination of water and hydrogen abstraction. First, ion **15** rearranges to yield ion **18** via **TS(15→18)**. This process is a hydrogen shift and requires a large amount of energy, since **TS(15→18)** is 4.28 eV above parent ion **1**. Ions **18** and **15** have comparable stabilities. Subsequently, ion **18** has its three-member ring opened via
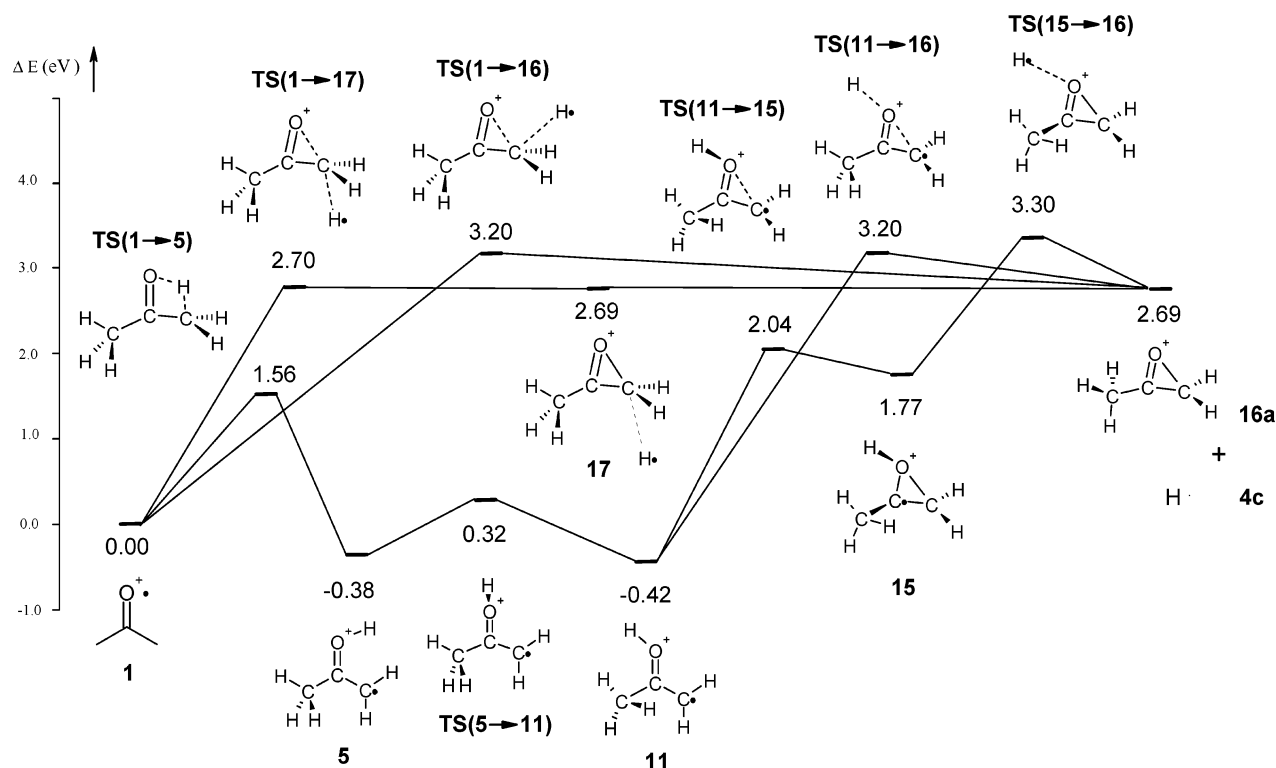
Figure 11. Gaussian-3 potential energy surface showing the possible mechanism for reaction 4, $CH_3COCH_3^+ \rightarrow CH_3COCH_2^+ + H$.

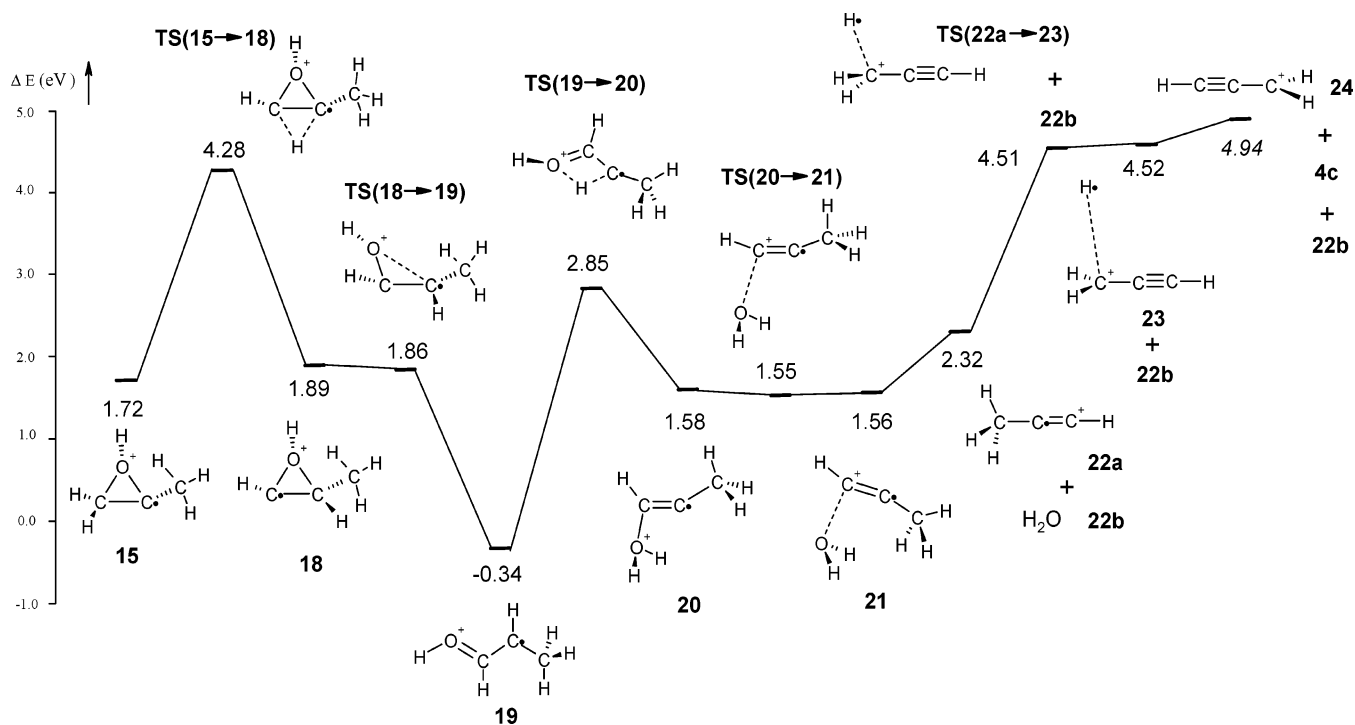**Figure 12.** Gaussian-3 potential energy surface showing the possible mechanism for reaction 5, $CH_3COCH_3^+ \rightarrow C_3H_3^+ + H_2O + H$. The energy sum of **22**, **4c**, and **20b** is calculated at the CCSD(T)/G3large level (see text).

TS(18→19). The G3 energy of **TS(18→19)** is lower than that of **18** by 0.03 eV, as the energy barrier involved is likely to be very low that it is within the error bar of the G3 method. Ion **19** has C_s symmetry and extensive π electron delocalization. Hence it is very stable. Ion **19** then undergoes H atom transfer via **TS(19→20)** to form **20**, where the short C–C bond has considerable triple bond character, and the C–C–C bond angle (156.1°) is exceedingly large. Ion **20** then undergoes a facile dissociation of water molecule via **TS(20→21)** to form INC

21, which subsequently dissociate the water molecule completely to yield $HCCCH_3^+$ (**22a**) and H_2O (**22b**). Cation **22a** then undergoes a couple of very facile process to yield the final product $HCCCH_2^+$ (**24**) and the other products H (**4c**) and H_2O (**22b**). The overall G3 dissociation energy for this rather complex dissociation channel is 4.53 eV, in only fair agreement with the experimental result of 4.82 ± 0.03 eV. In view of this relatively poor agreement between the G3 and experimental dissociation energies, we also carried out CCSD(T) calculations

Photoionization Study of Acetone

J. Phys. Chem. A, Vol. 109, No. 19, 2005 **4241**

employing the 6-31G(d) and G3large basis set for this dissociation energy. When no ZPVE correction is taken account, the CCSD(T)/6-31G(d) and CCSD(T)/G3large dissociation energies are 5.18 and 4.94 eV, respectively. After the inclusion of ZPVE corrections, the dissociation energies become 4.68 and 4.44 eV, respectively. So, once again, this proposed dissociation channel has computational support.

Before closing, it should be mentioned that the channels of reactions 1a and 2a have been studied theoretically with the MP2(Full) method using a number of basis sets by Anand and Schlegel.[28] In addition, these same two reactions have also been studied by Lin et al. using the Gaussian-2 method.[29]

Conclusion

We have measured the IE of acetone as well as the AEs of fragment ions CH_3^+, $C_2H_3^+$, $C_3H_3^+$, $C_3H_5^+$, CH_2CO^+, CH_3CO^+, and $CH_3COCH_2^+$ in the dissociative photoionizations of acetone by the combined techniques of synchrotron radiation, molecular beam and mass spectrometry. With the aid of ab initio G3 results, we have established the dissociation channels for the formation of the fragment ions CH_3CO^+, CH_2CO^+, CH_3^+, $C_3H_3^+$, and $CH_3COCH_2^+$ The agreements between the G3 and experimental results range from fair to excellent.

References and Notes

(1) Kanomata, I. *Bull. Chem. Soc. Jpn.* **1961**, *34*, 1864.
(2) Dorman, F. H. *J. Chem. Phys.* **1965**, *42*, 65.
(3) Shigorin, D. N.; Filyugina, A. D.; Potapov, V. K. *Teor. Eksperim. Khim.* **1966**, *2*, 554.
(4) Mouvier, G.; Hernndez, R. *Org. Mass Spectrom.* **1975**, *10*, 958.
(5) Watanabe, K. *J. Chem. Phys.* **1954**, *22*, 1564.
(6) Hurzeler, H.; Inghram, M. G.; Morrison, J. D. *J. Chem. Phys.* **1958**, *28*, 76.
(7) Murad, E.; Inghram, M. G. *J. Chem. Phys.* **1964**, *40*, 3263.
(8) Murad, E.; Inghram, M. G. *J. Chem. Phys.* **1964**, *41*, 404.
(9) Staley, R. H.; Wieting, R. D.; Beauchamp, J. L. *J. Am. Chem. Soc.* **1977**, *99*, 5964.
(10) Trott, W. M.; Blais, N. C.; Walters, E. A. *J. Chem. Phys.* **1978**, *69*, 3150.
(11) Traeger, J. C.; McLouglin, R. G.; Nicholson, A. J. C. *J. Am. Chem. Soc.* **1982**, *104*, 5318.
(12) Powis, I.; Danby, C. J. *Int. J. Mass. Spectrom. Ion Phys.* **1979**, *32*, 27.
(13) Qi, F.; Sheng, L.; Zhang, Y.; Yu, S.; Li, W.-K. *Chem. Phys. Lett.* **1995**, *234*, 450.
(14) Sheng, L.; Qi, F.; Tao, L.; Zhang, Y.; Yu, S.; Wong, C.-K.; Li, W.-K. *Int. J. Mass. Spectrom. Ion Process.* **1995**, *148*, 179.
(15) Sheng, L.; Qi, F.; Gao, H.; Zhang, Y.; Yu, S.; Li, W.-K. *Int. J. Mass. Spectrom. Ion Process.* **1997**, *161*, 151.
(16) Li, Q.; Ran, Q.; Chen, C.; Yu, S.; Ma, X.; Sheng, L.; Zhang, Y.; Li, W.-K. *Int. J. Mass. Spectrom. Ion Process.* **1996**, *153*, 29.
(17) Liu, F.; Qi, F.; Gao, H.; Sheng, L.; Zhang, Y.; Yu, S.; Lau, K.-C.; Li, W.-K. *J. Phys. Chem. A* **1999**, *103*, 4155.
(18) Lau, J. K.-C.; Li, W.-K.; Qi, F.; Suits, A. G. *J. Phys. Chem. A* **2002**, *106*, 11025.
(19) Law, C.-K.; Chien, S.-H.; Li, W.-K.; Cheung, Y.-S. *J. Phys. Chem. A* **2002**, *106*, 11271.
(20) Lee, H.-L.; Li, W.-K.; Chiu, S.-W. *J. Mol. Struct. (THEOCHEM)* **2003**, *620*, 107.
(21) Cheng, M.-F.; Li, W.-K. *J. Phys. Chem. A* **2002**, *106*, 11025.
(22) Lee, H.-L.; Li, W.-K.; Chiu, S.-W. *J. Mol. Struct. (THEOCHEM)* **2003**, *629*, 237.
(23) Frisch, M. J.; Trucks, G. W.; Schlegel, H. B.; Scuseria, G. E.; Robb, M. A.; Cheeseman, J. R.; Montgomery, J. J. A.; Vreven, T.; Kudin, K. N.; Burant, J. C.; Millam, J. M.; Iyengar, S. S.; Tomasi, J.; Barone, V.; Mennucci, B.; Cossi, M.; Scalmani, G.; Rega, N.; Petersson, G. A.; Nakatsuji, H.; Hada, M.; Ehara, M.; Toyota, K.; Fukuda, R.; Hasegawa, J.; Ishida, M.; Nakajima, T.; Honda, Y.; Kitao, O.; Nakai, H.; Klene, M.; Li, X.; Knox, J. E.; Hratchian, H. P.; Cross, J. B.; Bakken, V.; Adamo, C.; Jaramillo, J.; Gomperts, R.; Stratmann, R. E.; Yazyev, O.; Austin, A. J.; Cammi, R.; Pomelli, C.; Ochterski, J. W.; Ayala, P. Y.; Morokuma, K.; Vot, G. A.; Salvador, P.; Dannenberg, J. J.; Zakrzewski, V. G.; Dapprich, S.; Daniels, A. D.; Strain, M. C.; Farkas, O.; Malick, D. K.; Rabuck, A. D.; Raghavachari, K.; Foresman, J. B.; Ortiz, J. V.; Cui, Q.; Baboul, A. G.; Clifford, S.; Cioslowski, J.; Stefanov, B. B.; Liu, G.; Liashenko, A.; Piskorz, P.; Komaromi, I.; Martin, R. L.; Fox, D. J.; Keith, T.; Al-Laham, M. A.; Peng, C. Y.; Nanayakkara, A.; Challacombe, M.; Gill, P. M. W.; Johnson, B.; Chen, W.; Wong, M. W.; Gonzalez, C.; Pople, J. A. G*aussian 03*, Revision B. 05 ed.; Gaussian, Inc.: Wallingford CT, 2004.
(24) Walters, E. A.; Clay, J. T.; Grover, J. R. *J. Phys. Chem. A* **2005**, *109*, 1541.
(25) Chupka, W. A. *J. Chem. Phys.* **1959**, *30*, 191.
(26) McAdoo, D. J. *Mass Spectrom. Rev.* **1988**, *7*, 363.
(27) Chiu, S.-W.; Lau, J. K.-C.; Li, W.-K. *J. Phys. Chem. A* **2001**, *105*, 432.
(28) Anand, S.; Schlegel, H. B. *Phys. Chem. Chem. Phys.* **2004**, *6*, 5166.
(29) Mishima, K.; Hayashi, M.; Lin, S. H. *Int. J. Mass Spectrom.* **2004**, *238*, 1.